arXiv:cond-mat/0209566v1 [cond-mat.mes-hall] 24 Sep 2002

"Reservoir model" for shallow modulation-doped digital magnetic quantum wells

Henrique J. P. Freire[1,*] and J. Carlos Egues[2,†]

[1]Departamento de Física e Informática, Instituto de Física de São Carlos,
Universidade de São Paulo, Caixa Postal 369, 13560-970 São Carlos-SP, Brazil
[2]Department of Physics and Astronomy, University of Basel,
Klingelbergstrasse 82, CH-4056 Basel, Switzerland

(Dated: July 13, 2002)

Digital Magnetic Heterostructures (DMH) are semiconductor structures with magnetic monolayers. Here we study electronic and magneto-transport properties of shallow modulation-doped (ZnSe/ZnCdSe) DMHs with spin-5/2 Mn impurities. We compare the "reservoir" model, possibly relevant to shallow geometries, to the usual "constant-density" model. Our results are obtained by solving the Kohn-Sham equations within the Local Spin Density Approximation (LSDA). In the presence of a magnetic field, we show that both models exhibit characteristic behaviors for the electronic structure, two-dimensional carrier density, Fermi level and transport properties. Our results illustrate the relevance of exchange and correlation effects in the study shallow heterostructures of the group II-VI.

Keywords: digital magnetic heterostructures, spin-polarized magneto transport, magnetic semiconductors, DFT/LSDA.

Digital Magnetic Heterostructures (DMHs) are state of the art layered semiconductor structures in which (quasi-)two-dimensional distributions of magnetic moments are restricted to equidistant planes within a quantum well [1, 2]. Spin-dependent quantum effects are pronounced in these systems. For example, in an external magnetic field the s-d exchange interaction [3] between itinerant electrons and those of the magnetic impurities is responsible for a giant Zeeman effect up to two orders of magnitude larger than the ordinary one. These large energy splittings are readily observed by magneto-photoluminescence [1, 4]. In addition, the successful achievement of high-doping carrier densities in [5] has enabled magnetotransport and magneto-photoluminescence measurements in these systems [6, 7, 8].

In this work we investigate spin-dependent properties of shallow DMHs, Fig. 1(a). "Shallow" here implies that the confining potential is weak enough, e.g. 25 meV for a 10.5 nm wide well [Fig. 1(b)], so as to have only a few confined subbands. For such geometries, the adjacent n-doped regions with densities 10^{17} cm^{-3} provide enough carriers to fill up all confined levels in the well, thus serving as electron reservoirs. We describe these shallow DMHs using a "reservoir model" with a constant Fermi level pinned to the chemical potential of the n-doped regions [9, 10]. Such a model has also been applied to GaAs/GaAlAs [11, 12, 13] and to ZnSe/ZnCdSe [14] systems. We calculate the magnetic-field dependent subband structure of our shallow DMHs by using Density Functional Theory within a Local Spin Density Approximation (DFT/LSDA). As recently shown, exchange-correlation effects are important in shallow II-VI wells [15]. We determine Landau-level fan diagrams, two-dimensional electron densities, and in-plane transverse resistivities.

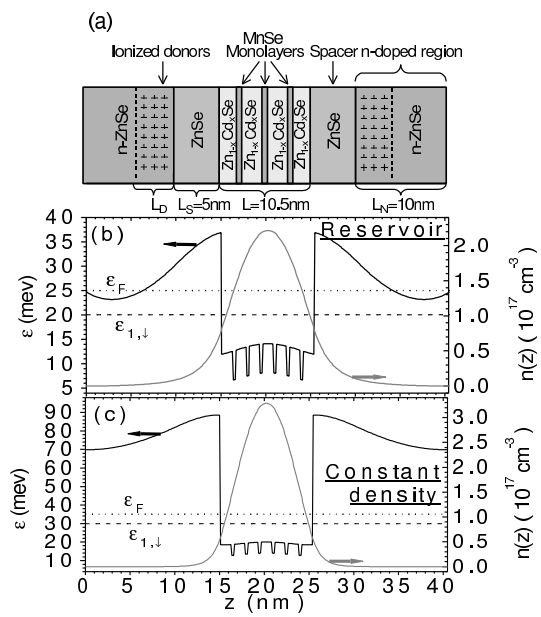

FIG. 1: (a) Layered structure of a digital magnetic quantum well heterostructure. Lateral n-doped regions (impurity concentration of 1-2 10^{17} cm^{-3}) provide electrons that fill the confined energy levels. Self-consistent potential profile for majority spin down electrons (at B = 1 T) are shown for the "reservoir" (b) and "constant density" (c) regimes. Each case has only one confined subband bellow the Fermi level. In (b) total electronic density n(z) penetrates into the lateral barriers allowing exchange and correlation to contribute to the potential profile far from the well center.

*Electronic address: freire@if.sc.usp.br
†Electronic address: carlos.egues@unibas.ch

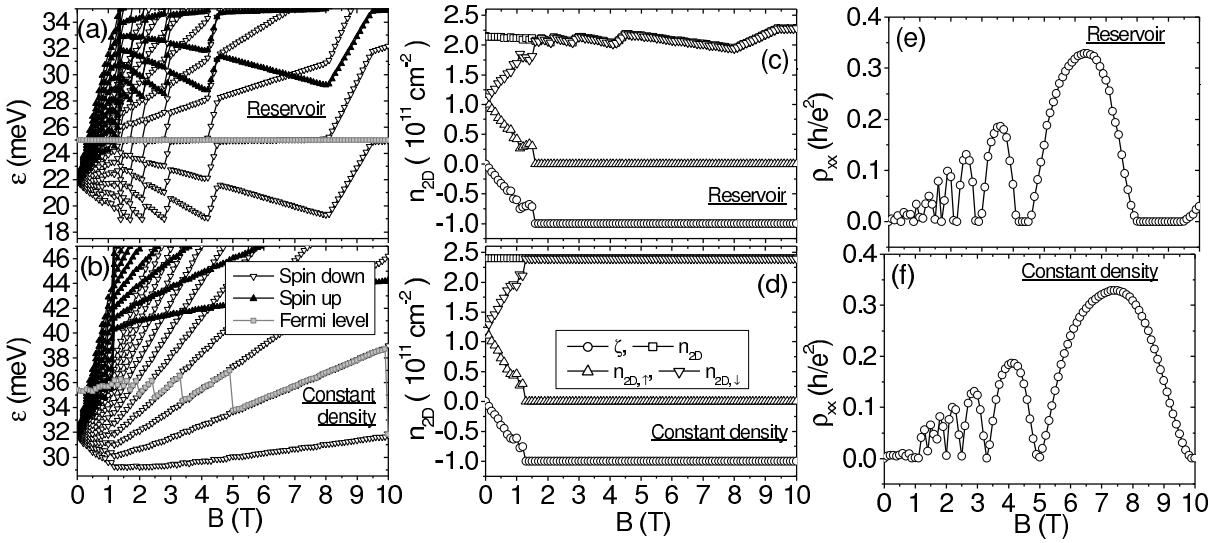

FIG. 2: Magnetic field dependence of calculated Landau levels, two-dimensional densities, and transverse resistivities for both the reservoir (upper panels) and the constant density (lower panels) models. Within the reservoir model the Landau levels (a) are pinned to the Fermi level ε_F of the reservoirs, thus originating sawtooth-profile LL fan diagrams. ε_F (b) is pinned to the highest occupied LL in the constant-density model and oscillates as the magnetic field is increased. The s-d enhanced LL spin splitting gives rise to the spin polarization of the 2DEG at low B fields [(c) and (d)]. Note the oscillatory behavior of the two-dimensional density within the reservoir model (c). The transverse resisitivities ρ_{xx} display Shubnikov-de Haas oscillations in both regimes (e) and (f); however, plateaus $\rho_{xx} = 0$ are seen only in (e) since we do not account for localized states in this model.

We compare our results within the "reservoir model" with those obtained with the conventional "constant-density" model, in which deep enough wells can confine all available carriers. In this case the n-doped regions adjacent to the well are fully depleted. We configure the system geometry for each case by suitably choosing the height of the confining barriers at the ZnSe/(Zn,Cd)Se interfaces: 70 meV and 25 meV for the "constant density" and the "reservoir" models, respectively. The idea is to identify relevant contrasting features in these models to eventually better describe real shallow DMHs.

We calculate the magnetic-field dependent subband structure of our system within Density Functional Theory (DFT). We solve the Kohn-Sham (KS) equations in the Local Spin Density Approximation (LSDA) using the parametrization of VWN [16]. We compare our LSDA results to those obtained within the Hartree approximation to assess the role of exchange and correlation (XC) effects in the properties of these novel systems. We consider the system at zero temperature and perform the calculations in the effective-mass approximation framework. We also make the usual assumption that we can interpret the resulting KS eigenvalues as subband energies of the system. Consequently, the total energy of each Landau level (LL) is the sum of the subband energy $\varepsilon_{i,z}$ and the Landau cyclotron energy $(n + 1/2)\hbar\omega_c$

$$\varepsilon_{i,n,z}(B) = \varepsilon_{i,z}(B) + \left(n + \frac{1}{2}\right)\hbar\omega_c + \frac{1}{2} g \mu_B B_z : \quad (1)$$

In (1), the subband energy $\varepsilon_{i,z}(B)$ corresponds to the longitudinal confined electronic motion and the second term to the quantized transversal motion due to the magnetic field. For completeness we also add the Zeeman energy, although its contribution is very small when compared to the s-d exchange interaction.

Panels (b) and (c) of Fig. 1 show the resulting self-consistent potential profiles for both "reservoir" (a) and "constant-density" (b) regimes. As the magnetic field increases, the self-consistent potential and the corresponding electronic structure change due to i) magnetic-field dependent contributions to the confining potential and ii) the rearrangement of electrons in the confined levels (magnetic-field dependent Landau-level degeneracy eB/h).

Figures 2(a) and (b) show the Landau-level fan diagrams for both regimes and the magnetic field dependence of the Fermi energy ε_F. In the "reservoir" regime case the Fermi level is constant at the chemical potential of the reservoir (n-doped regions) while in the "constant density" case ε_F oscillates as a function of B. In the first case, all confined electronic levels are fully occupied because n-doped regions can always provide enough electrons to the QW, thus being only partially depleted. For this reason the LLs are pinned to the Fermi level (see plateaus at ε_F). In the "constant density" case the n-doped regions are completely depleted but the amount of electrons provided to the QW is not sufficient to fill all electronic levels. Consequently, the Fermi energy is

pinned to the highest occupied LL, and oscillates as a function of the magnetic field [Fig. 2(b)]. Note that in this case ε_F is pinned to the LL, not the contrary as in the "reservoir" regime. This is why the curves in former case exhibit a sawtooth profile not present in the latter. Note also that in the "reservoir" ("constant density") case the two-dimensional density n_{2D} changes (is constant) as a function of B [Fig. 2(c) and (d)].

When compared to pure Hartree calculations (c.f. Ref. [15]) we note that XC plays an important role in such group II-VI heterostructures. Within LSDA calculations the LL spin splitting is enhanced, the two-dimensional density is increased, and the magnetic field at which the 2DEG becomes fully polarized is decreased.

We also calculate the magnetic field dependence of the in-plane resistivities (perpendicular to the magnetic field and growth axis). We use Ando's model for the longitudinal conductivity $_{xx}$ [17] and Drude's model for the transversal component of the conductivity, $_{xy} = en_{2D}/B$. These simple models enable us to illustrate general magnetotransport features within these n-doped magnetic structures and to compare the two regimes for the density. In Fig. 2(e) and (f) we plot our results for the in-plane longitudinal resistivity (= ^{1}) which is a relevant experimental quantity.

Both "reservoir" and "constant density" regimes display the usual oscillations in $_{xx}$ (Shubnikov-de Haas oscillations), but the former has regions of zero resistivity [Fig. 2(e)]. In the "reservoir" regime the QW is always filled with the maximum number of electrons possible, which is defined by both the magnetic-field dependent density of states and the reservoir chemical potential. Within this self-consistent equilibrium, there are magnetic field ranges at which the center of the LLs are not on the Fermi level [Fig. 2(a)], and consequently, the resistivity is minimum [Fig. 2(e)]. In the "constant density" case, on the other hand, the Fermi level is always pinned to highest occupied LL and the minimum resistivity dips [Fig. 2(f)] occur at magnetic fields that ε_F jumps between LLs [Fig. 2(b)]. At those magnetic fields, ε_F lies on the tail of a LL [18] so that there is only a small number of conducting electrons and, consequently, a correspondingly small resistivity. In passing, we note that in the standard model for the integer quantum hall effect (IQHE) [19], localized states in broadened LLs are responsible for the Fermi-level pinning [20]; the phenomenological inclusion of these states (gaussian density of states) gives rise to plateaus $_{xx} = 0$.

Finally, we should mention that we are currently investigating the temperature dependence of the transverse magnetoresistivity [21]; a more detailed analysis, beyond the scope of this communication, will be addressed in a future publication. This additional study should allow us to contrast the two models discussed here in terms of agreement with experimental data.

The authors thank Klaus Capelle for useful discussions. JCE acknowledges support from the Swiss NSF, NCCR Nanoscience, DARPA, and ARO. HJPF acknowledges financial support from FAPESP (Brazil).

[1] S. Crooker et al., Phys. Rev. Lett. 75, 505 (1995).
[2] D. D. Awschalom and N. Samarth, J. Magn. Magn. Mater. 200, 130 (1999).
[3] J. K. Furdyna, J. Appl. Phys. 64, R29 (1988).
[4] See J. C. Egues and J. W. Wilkins, Phys. Rev. B 58, R16012 (1998) for a theoretical calculations of exchange splitting and spin-flip times in DMHs.
[5] I. P. Smorchkova and N. Samarth, Appl. Phys. Lett. 69, 1640 (1996).
[6] I. P. Smorchkova, N. Samarth, J. M. Kikkawa, and D. D. Awschalom, Phys. Rev. Lett. 78, 3571 (1997).
[7] Longitudinal magnetotransport in Mn-based heterostructures has also been recently achieved. See, for instance, R. Fiederling et al., Nature (London) 402, 787 (1999); Y. Ohno et al., Nature (London) 402, 790 (1999). See also G. Schmidt et al., Phys. Rev. Lett. 87, 227203 (2001).
[8] For theoretical works on longitudinal spin-polarized transport see J. C. Egues, Phys. Rev. Lett. 80, 4578 (1998); J. C. Egues, C. Gould, G. Richter, and L. W. Molenkamp, Phys. Rev. B 64, 195319 (2001); K. Chang and F. M. Peeters, Solid State Commun. 120, 181 (2001); and Y. Guo, J. Lu, B. Gu, and Y. Kawazoe, Phys. Rev. B 64, 155312 (2001).
[9] G. A. Baraff and D. C. Tsui, Phys. Rev. B 24, 2274 (1981).
[10] A. Raymond and H. Sibari, Phys. Stat. Sol. (b) 183, 159 (1994).
[11] M. V. der Burgt et al., Phys. Rev. B 52, 12218 (1995).
[12] Y. Takagaki, K. Muraki, and S. Tarucha, Phys. Rev. B 56, 1057 (1997).
[13] A. Raymond et al., Semicond. Sci. Technol. 14, 915 (1999).
[14] S. P. Hong, K. S. Yi, and J. J. Quinn, Phys. Rev. B 61, 13745 (2000).
[15] H. J. P. Freire and J. C. Egues, Braz. J. Phys. 32, 327 (2002); cond-mat/0112263 (2001).
[16] S. H. Vosko, L. Wilk, and M. Nusair, Can. J. Phys. 58, 1200 (1980).
[17] T. Ando and Y. Uemura, J. Phys. Soc. Japan 36, 959 (1974).
[18] We actually simulate discrete Landau levels by using very narrow (0.004 meV) gaussian-shaped profiles in the density of states. Consequentely, $_{xx}$ in Fig. 2(e) and (f) have a smooth oscilatory behavior.
[19] K. V. Klitzing, G. Dorda, and M. Pepper, Phys. Rev. Lett. 45, 494 (1980).
[20] H. L. Stormer and D. C. Tsui, Science 220, 1241 (1983).
[21] R. Knobel, N. Samarth, J. G. E. Harris, and D. D. Awschalom, Phys. Rev. B 65, 235327 (2002); J. G. E. Harris et al., Phys. Rev. Lett. 86, 4644 (2001).